

SUPERMASSIVE BLACK HOLES IN ACTIVE GALACTIC NUCLEI. I. THE CONSISTENCY OF BLACK HOLE MASSES IN QUIESCENT AND ACTIVE GALAXIES.

LAURA FERRARESE,^{1,2} RICHARD W. POGGE,^{2,3} BRADLEY M. PETERSON,^{2,3} DAVID MERRITT,¹
 AMRI WANDEL,⁴ AND CHARLES L. JOSEPH¹

Submitted to the Astrophysical Journal Letters

ABSTRACT

We report the first results of a program to measure accurate stellar velocity dispersions in the bulges of the host galaxies of active galactic nuclei (AGNs) for which accurate black hole (BH) masses have been determined via reverberation mapping. We find good agreement between BH masses obtained from reverberation mapping, and from the $M_\bullet - \sigma$ relation as defined by quiescent galaxies, indicating a common relationship between active and quiescent black holes and their larger-scale environments.

Subject headings: galaxies: active — galaxies: Seyfert

1. INTRODUCTION

Two techniques have been successfully applied over the last few years to derive masses of supermassive black holes (BHs) in samples of galaxies. Kinematics of stars or gas on scales of $\lesssim 1 - 10$ pc yield estimates of M_\bullet based on Newton's laws under the assumption that the observed motions reflect the gravitational influence of the BH. This technique has been applied to galaxies near enough ($d \lesssim 100$ Mpc) that the radius of influence of the BH, $r_h = GM_\bullet/\sigma_\star^2$, is likely to have been resolved on the angular scales accessible to ground- and space-based telescopes, $1'' \gtrsim \theta \gtrsim 0''.1$. The second technique, "reverberation mapping" (RM), makes use of broad emission-line variability to estimate BH masses in active galactic nuclei (AGNs). The size of the broad emission-line region is estimated from time delays between variations in the continuum (assumed to originate near the BH) and the response of the broad emission lines (Blandford & McKee 1982; Peterson 1993; Netzer & Peterson 1997). By combining the time delays with the emission-line widths, the BH mass then follows from the virial theorem. Black hole masses based on RM have been published for about three dozen AGNs (Wandel, Peterson & Malkan 1999; Kaspí et al. 2000).

Both mass-estimation techniques have strengths and weaknesses. Masses derived from RM are based on gas that is much closer to the BH, often $r \lesssim 0.01$ pc, than the stars or gas used in kinematical studies. At these separations, the gravitational force to which the gas responds is due almost entirely to the BH and there is little danger of a "false detection." However the precise relation between M_\bullet and the measured quantities is uncertain at levels of $\sim 50\%$ due primarily to uncertainties in the geometry and kinematics of the BLR and other unknowns (e.g., Krolik 2001).

In the case of BH masses derived from spatially resolved kinematics, formal accuracies can be high provided r_h has actually been resolved; otherwise, estimates of M_\bullet depend sensitively on assumptions about the character of the motion near the BH. Here the danger is that the inferred BH mass is actually

a measure of the *combined* mass of the BH and the stars in the resolved region, $r \gg r_h$; modeling techniques applied to such data can substantially overestimate M_\bullet by ascribing too much of the gravitational force in the nucleus to the BH and too little to the stars.

In fact, there have been claims of systematic differences between RM and kinematical BH masses, in the sense that RM masses at a given bulge luminosity, M_B , are a factor ~ 20 smaller than kinematical masses (Wandel 1999). The discrepancy has most often been ascribed to systematic errors in the RM masses (Richstone et al. 1998; Faber 1999; Ho 1999). Unfortunately, it is extremely difficult to make a direct comparison between dynamical and reverberation-based BH masses. In AGNs, the variable nonstellar continuum and broad emission lines that enable RM tend to swamp the stellar features at $r < r_h$ which are needed to study the stellar dynamics. At the present time, there is no galaxy for which the BH mass has been measured using both techniques.

A possible solution to this problem emerged with the discovery of the $M_\bullet - \sigma$ relation, a tight empirical correlation between M_\bullet and the stellar velocity dispersion σ (Ferrarese & Merritt 2000, hereafter FM00; Gebhardt et al. 2000a, hereafter G00a). The latter is defined on scales much larger than r_h and hence is easily accessible to ground-based instruments. Since stellar velocity dispersions can also be measured in active galaxy hosts, it is possible to determine whether the $M_\bullet - \sigma$ relation for AGNs is similar to that of quiescent galaxies. Preliminary attempts at such a comparison have been published (Gebhardt et al. 2000b [hereafter G00b]; Merritt & Ferrarese 2001a [hereafter MF01a]) based on published AGN bulge velocity dispersions (principally from Nelson & Whittle 1995, hereafter NW95). These studies reveal a general consistency between the AGN data and the $M_\bullet - \sigma$ relation for normal galaxies, confirming that the apparent discrepancies between the kinematic and RM masses were due mostly to systematic overestimates in the BH masses derived from stellar kinematic measurements (MF01a,

¹Department of Physics and Astronomy, Rutgers University, New Brunswick, NJ 08854
 lff@physics.rutgers.edu, merritt@physics.rutgers.edu, cjoseph@physics.rutgers.edu

²Visiting Astronomer, Kitt Peak National Observatory, National Optical Astronomy Observatories, which is operated by the Association of Universities for Research in Astronomy, Inc. (AURA), under a cooperative agreement with the National Science Foundation.

³Department of Astronomy, The Ohio State University, 140 West 18th Avenue, Columbus, OH 43210
 peterson@astronomy.ohio-state.edu, pogge@astronomy.ohio-state.edu

⁴Racah Institute, Hebrew University, Jerusalem 91904, Israel
 amri@frodo.fiz.huji.ac.il

Merritt & Ferrarese 2001b). Unfortunately, the uncertainties in both the AGN BH masses and stellar velocity dispersions used by G00b and MF01a are too large to provide a truly critical test. The reason for the large uncertainties in M_\bullet is quite simple: the largest source of random errors in AGN BH masses is the light-travel time delay for the emission lines, which determines the size of the line-emitting region. The fractional error in this quantity is largest for those sources that have the smallest line-emitting regions, since the uncertainties are determined in large part by the time resolution of the monitoring program. The smallest line-emitting regions are found in the least-luminous objects (i.e., $R \propto L^{0.5-0.7}$; Kaspi et al. 2000). Generally speaking, lower-luminosity AGNs have not been monitored any more closely than higher-luminosity AGNs and thus the fractional errors in their BH masses are relatively large, in some cases as large as 100%. The low-luminosity AGNs are the very galaxies for which bulge velocity dispersions have been measured, and thus do not yet provide a conclusive argument for consistency between the $M_\bullet - \sigma$ relations in AGNs and normal galaxies.

In order to better compare the $M_\bullet - \sigma$ relations for AGNs and quiescent galaxies, we are undertaking a program to measure bulge velocity dispersions of the host galaxies of AGNs with formally well-determined reverberation-based BH masses. In this contribution, we describe the first results from this program.

2. OBSERVATIONS AND DATA REDUCTION

2.1. Sample Selection

Black hole masses based on reverberation studies have been published for 34 AGNs (Wandel, Peterson & Malkan 1999; Kaspi et al. 2000). There are both systematic and random uncertainties in these measurements: systematic errors arise primarily from the largely unknown geometry and kinematics of the line-emitting region, and the random errors are due mostly to uncertainties in the size of the line-emitting region, as noted earlier, and the uncertainty in the translation of the observed FWHM to the 3-D velocity dispersion. The typical level of random uncertainty in the reverberation-based BH masses is $\gtrsim 50\%$. We focus our attention on those AGNs with better-determined BH masses (i.e., smaller random errors). These provide the most meaningful comparison with normal galaxies: the scatter in the $M_\bullet - \sigma$ relation for normal galaxies is $\sim 30\%$, while the intrinsic scatter in the relation appears to be negligible (FM00).

2.2. Observations

We have obtained bulge velocity dispersions from the CaII triplet lines at rest wavelengths 8498, 8542, and 8662 Å. These lines are in the spectral region where the AGN contribution is minimized (e.g., NW95).

The objects observed in this study are listed in Table 1. Column (1) gives the common name of the object, and its redshift is given in column (2). Column (3) gives the reverberation-based virial mass of the central BH in each object, and the published source of the virial mass is given in column (4).

The observations reported here were obtained on UTC 2001 April 7–9 on the Mayall 4-m Telescope of the National Optical Astronomy Observatories on Kitt Peak. The observations were made with the Ritchey-Chretien Spectrograph with the BL380 grating (1200 lines per mm, blazed at 9000 Å, centered at approximately 8910 Å), and an RG610 blocking filter.

The detector employed was the T2KB CCD, a back-illuminated 2048×2048 device windowed to 440×2048 pixels. The slit width was set to $2''$. The resulting spectra have a resolution $R \approx 5000$, and cover the range 8150–9660 Å. To allow accurate sky-subtraction, a long slit ($\sim 5'$) was used. Column (5) of Table 1 gives the spectrograph position angle at which the observations were made; when such information was available, we aligned the slit along the major axis of the galaxy. Column (6) gives the total integration time on each source.

Each observation of a galaxy was bracketed with quartz-lamp spectra for flat-field correction, and He-Ne-Ar spectra for wavelength calibration. A spectrum of the twilight sky was obtained to determine a nightly cross-dispersion illumination correction. We also obtained spectra of 14 late-type giant stars (G8 III — K6 III) that were used as templates and radial-velocity standards in the analysis described below.

2.3. Data Reduction

The raw long-slit spectra were reduced by flat-field, bias, and slit-illumination corrections following the procedures described by Pogge (1992). We used the XVISTA⁵ package for all reductions. Curvature of the long-slit spectra in the dispersion and cross-dispersion directions was removed by tracing stars and bright, isolated night-sky emission lines in the spectra and rectifying the long-slit spectra. In this spectral region, the T2KB CCD is subject to fringing at the 10% level longward of ~ 9000 Å, which we reduced by using the bracketing flat-field exposures. In general, residual fringing was less than 0.1% in the spectral regions of interest. We combined the longslit spectra in groups of three 20-min exposures to remove cosmic-ray events by sigma clipping with a simple CCD noise model (gain = 1.9 e^- , $\sigma_{\text{read-out}} = 5 \text{ e}^-$). The nuclear spectra were extracted from each group within a $2'' \times 4''$ aperture centered on the nucleus. For the fainter objects, we used a $4''.8$ extraction aperture to improve the signal-to-noise ratio. Sky spectra were extracted from flanking regions along the slit and subtracted from the nuclear spectra. We then combined all of the nuclear spectra into a final spectrum. This group-wise extraction of spectra taken within at most an hour of each other reduced the effects of variability in the atmospheric OH airglow lines. The fully reduced spectra of all objects are shown in Fig. 1.

We point out that the $M_\bullet - \sigma$ relation was defined by FM00 using central velocity dispersions corrected to an aperture of size $r_e/8$, with r_e the effective radius of the galaxy. G00a, on the other hand, used spatially averaged, rms, line-of-sight velocity dispersion within r_e . MF01a demonstrated that there is no systematic difference between the two definitions of σ in this sample. The bulge effective radius is not known for any of our target galaxies, but the bulge is enclosed within the aperture used for the spectral extraction. On this basis, in §3 we treat our measured dispersions on the same basis as the aperture-corrected dispersions tabulated by MF01a.

2.4. Data Analysis

Two independent estimates of the stellar velocity dispersion were obtained from the Ca II triplet. The first employed the Fourier Correlation Quotient (FCQ) method described by Bender (1990) and Bender, Saglia, and Gerhard (1994). The second was based on the Maximum Penalized Likelihood (MPL) method developed by Merritt (1997). FCQ and MPL differ in

⁵See <http://ganymede.nmsu.edu/holtz/xvista>.

TABLE 1
AGN SAMPLE OBSERVED

Galaxy	Redshift	M_{\bullet}	Source ¹	Position	Exposure Time	$\sigma(\text{FCQ})$	$\sigma(\text{MPL})$
(1)	(2)	($10^7 M_{\odot}$)	(4)	Angle	(sec)	(km s^{-1})	(km s^{-1})
		(3)		(5)	(6)	(7)	(8)
NGC 4051	0.0024	$0.14^{+0.10}_{-0.06}$	1	135°	3600	80 ± 4	80 ± 3
NGC 4151	0.0033	$1.20^{+0.83}_{-0.70}$	2	135°	3600	93 ± 5	85 ± 5
NGC 5548	0.017	5.9 ± 2.5	3	110°	7200	183 ± 10	180 ± 6
Mrk 79	0.022	$10.2^{+3.9}_{-5.6}$	2	56°	7200	130 ± 9	120 ± 8
Mrk 110	0.036	$0.77^{+0.38}_{-0.29}$	2	110°	15600	86 ± 5	95 ± 8
Mrk 817	0.031	$3.54^{+1.03}_{-0.86}$	2	90°	12000	142 ± 6	140 ± 8

¹Data source for masses: 1: Peterson et al. (2000); 2: Kaspi et al. (2000); 3: Peterson & Wandel (2000)

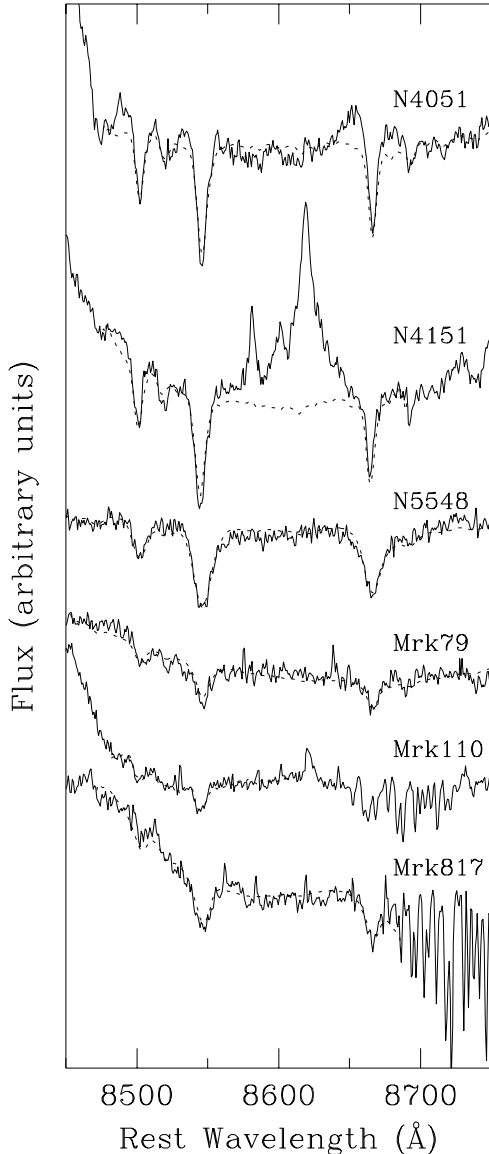


FIG. 1.— Calibrated spectra for the six galaxies in our program. An arbitrary additive constant has been added to the fluxes on the vertical axis. The dotted line represents the best fit returned by the FCQ method.

important ways (e.g., Joseph et al. 2001); using both allows us to assess the impact of systematics on the measured values. MPL was applied to the fully calibrated and continuum normalized spectra. FCQ incorporates a continuum fitting routine, thus was applied to the spectra before normalization. The velocity dispersion measurements resulting from FCQ and MPL are listed in columns (7) and (8) of Table 1, respectively. The errors associated with σ are the formal random uncertainties returned by the FCQ and MPL codes, but there are likely unaccounted systematic uncertainties. Repeating the analysis using different stellar templates, or changing the parameters for the continuum fits in FCQ show that a more realistic error estimate is of order 15%.

3. RESULTS AND DISCUSSION

No velocity dispersions have been previously published for Mrk79, Mrk110 and Mrk817. NW95 listed velocity dispersions from CaII and/or Mgb absorption lines for six galaxies with reverberation-based BH masses, including NGC4151 and NGC 5548. Unfortunately, NW95 warn that only for two of these galaxies, NGC 4051 and 3C120, are the measured dispersions deemed accurate. For NGC 4051, they quote $\sigma = 88 \pm 13 \text{ km s}^{-1}$, in good agreement with our result. For 3C120, which has a RM mass of $3.0^{+1.9}_{-1.4} \times 10^7 M_{\odot}$ (Wandel, Peterson & Malkan 1999; Kaspi et al. 2000) NW95 list $\sigma = 162 \pm 20 \text{ km s}^{-1}$ (from Smith, Heckman, & Illingworth 1990). For lack of an alternative, the NW95 velocity dispersions for all six galaxies were adopted by G00b and MF01a, in spite of their large associated uncertainties.

In Fig. 2, we show the relationship between BH mass and bulge velocity dispersion (FCQ values with 15% errors assumed) for the six galaxies listed in Table 1, along with the same relationship for quiescent or weakly active galaxies (full references for both M_{\bullet} and σ for the latter can be found in MF01a). For completeness, we also plot, as small open circles, the sample of galaxies for which values of M_{\bullet} were tabulated by G00a based on dynamical modeling of *Hubble Space Telescope* data, although we refrain from using these data in the following discussion since the modeling and analysis of the data that led to those M_{\bullet} measurements have yet to be published.

While secure conclusions are premature given the small sample size, several points are worth mentioning. As noted by

G00b and MF01a based on lower-quality data than presented in this paper, the current evidence is that reverberation-based masses are not systematically underestimated as suggested by, e.g., Richstone et al. (1998), Faber (1999) and Ho (1999). We stress that the data presented in this paper are unique for having high-quality measurements of both M_{\bullet} and σ . Our data support the conclusion that dynamical and reverberation-based masses are generally consistent, and that the two methods can potentially yield BH mass estimates of comparable precision. This is of particular relevance. Reverberation mapping is intrinsically unbiased with respect to BH mass, provided the galaxies can be monitored at closely spaced time intervals. While dynamical methods rely on the ability to spatially resolve the region dominated by the BH gravitational potential, RM samples a region which is per se unresolvable. It follows that an aggressive monitoring campaign of AGNs is the only viable method to probe the low-mass (M_{\bullet} less than a few million solar masses) end of the $M_{\bullet} - \sigma$ relation. It is also apparently as good a method as traditional dynamical studies to probe the higher-mass regime, although the obvious drawback is that it is perforce limited to galaxies with Type 1 AGN, which constitute only $\sim 1\%$ of the general galaxy population. Probing the low mass end of the $M_{\bullet} - \sigma$ relation is of particular interest since the slope and scatter of the relation have important implications for both hierarchical models of galaxy formation (Haehnelt, Natarajan, & Rees 1998; Silk & Rees 1998; Haehnelt & Kauffmann 2000) and the effect of mergers on the subsequent evolution (Cattaneo et al. 1999), including the coalescence of the binary BHs which are expected to form as a result of galaxy mergers (Milosavljevic & Merriitt 2001).

Furthermore, RM can probe galaxies at high redshift and with a wide range of nuclear activity, opening an avenue to explore possible dependences of the $M_{\bullet} - \sigma$ relation on redshift and activity level. Regarding the latter point, we note that NGC 4051, the galaxy with the smallest M_{\bullet} in our sample, is a narrow-line Seyfert 1 (NLS1) galaxy. Mrk 110 also approximately meets the traditional narrow-line Seyfert 1 criterion that $\text{FWHM}(\text{H}\beta) \leq 2000 \text{ km s}^{-1}$. The BH masses of the NLS1s are consistent with those of the other AGNs, and all are consistent with the masses inferred from the $M_{\bullet} - \sigma$ relation defined by the quiescent galaxies. This result is at odds with the recent findings of Mathur et al. (2001), who claim that NLS1s lie systematically below the $M_{\bullet} - \sigma$ relation defined by Seyfert 1 galaxies. One paradigm for NLS1s is that, compared to AGNs with similar non-thermal luminosity, they are powered by lower mass BHs accreting at a relatively higher accretion rate. A competing explanation is that they differ from other AGNs only in inclination; the small widths of the broad lines and concomitantly low reverberation masses are due to viewing disk-like sources at low inclination (i.e., nearly face-on). The consistency of the BH mass and bulge velocity dispersion of NGC 4051, in particular, with the $M_{\bullet} - \sigma$ relation for other galaxies strongly favors the low-mass/high accretion rate interpretation for the nature of NLS1s.

A linear fit to the sample of 18 galaxies — 12 galaxies from FM00 plus the six reverberation-mapped galaxies — using regression with bivariate errors and intrinsic scatter (Akritas & Bershady 1996; see also discussion in MF01a) gives a slope of

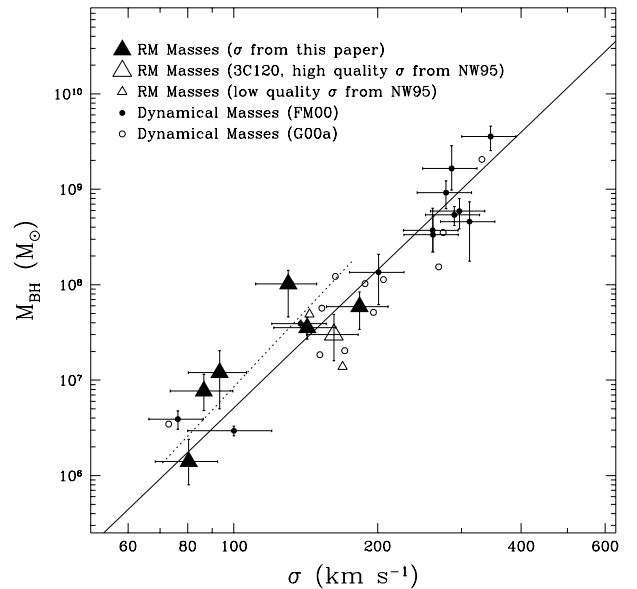


FIG. 2.— Black hole mass versus central velocity dispersion σ of the host elliptical galaxy or bulge. Small filled circles and errorbars represent quiescent or weakly active galaxies with dynamical measurements of M_{\bullet} . Open circles represent unpublished dynamical BH masses listed by G00a. Large solid triangles are the reverberation-mapped galaxies presented in this paper, while open triangles are reverberation-mapped galaxies for which σ is available in the literature. The solid line is the best linear fit to the $M_{\bullet} - \sigma$ relation as published by MF01a for the kinematical masses only (filled circles), with slope 4.81 ± 0.55 . The dotted line is the best fit to the six RM galaxies presented in this paper (filled triangles), and has a slope 5.3 ± 1.6 .

4.50 ± 0.34 , consistent with the slope of 4.81 ± 0.55 derived by MF01a using only the kinematical mass estimates. To conclude, we note that three of the galaxies in Fig. 2, NGC 4151, Mrk 79, and Mrk 110, seem to lie slightly above the “fiducial” $M_{\bullet} - \sigma$ relation defined by MF01a; i.e., these galaxies have black holes larger than expected from their bulge velocity dispersions. This is unlikely to be attributable to systematic errors in σ , since the quality of the fit returned by both FCQ and MPL for these galaxies, while not as good as for NGC 4051 and NGC 5548, is comparable to that of Mrk 817, which lies on the fiducial relation. There also seems to be no correlation between residuals and distance⁶. A more detailed discussion is premature at this point: the small discrepancy could be due to small systematic errors in the RM masses, or, perhaps more interesting, may indicate that the current level of activity has allowed for significant growth of the BH mass. These results underscore the importance of further testing the $M_{\bullet} - \sigma$ relation by measuring σ for a larger sample of reverberation-mapped galaxies over a large BH mass range.

We are grateful to NOAO for observing time on the 4-m telescope, and especially to H. Halbedel and B. Gillespie for capable assistance at the telescope. LF acknowledges NASA LTSA grant NAG5-8693. This research has made use of the NASA/IPAC Extragalactic Database (NED), which is operated by the Jet Propulsion Laboratory, California Institute of Technology, under contract with the National Aeronautics and Space Administration.

⁶Note that reverberation-mapping masses are independent of distance, therefore the scatter cannot be due to errors in the distance determination to these galaxies.

REFERENCES

- Akritis, M. G. & Bershad, M. A. 1996, *ApJ*, 470, 706
- Bender, R. 1990, *A&A*, 229, 441
- Bender, R., Saglia, R. P., & Gerhard, O. 1994, *MNRAS*, 269, 785
- Blandford, R., & McKee, C.F. 1982, *ApJ*, 255, 419
- Cattaneo, A., et al. 1999, *MNRAS*, 308, 77
- Faber, S.M. 1999, *Advances in Space Research*, 23, 925
- Ferrarese, L., & Merritt, D. 2000, *ApJ*, 539, L9 (FM00)
- Gebhardt, K., et al. 2000a, *ApJ*, 539, L13 (G00a)
- Gebhardt, K., et al. 2000b, *ApJ*, 543, L5 (G00b)
- Haehnelt, M., Natarajan, P., & Rees, M. 1998, *MNRAS*, 300, 817
- Haehnelt, M., & Kauffmann, G. 2000, *MNRAS*, 318, 35
- Ho, L.C. 1999, in *Observational Evidence for Black Holes in the Universe*, ed. S.K. Chakrabarti (Dordrecht: Reidel), p. 157
- Joseph, C.L., et al. 2001, *ApJ*, 550, 668
- Kaspi, S., Smith, P.S., Netzer, H., Maoz, D., Jannuzi, B.T., & Givon, U. 2000, *ApJ*, 533, 631
- Krolik, J., 2001, *ApJ*, in press (astro-ph/0012134)
- Mathur, S., Kuraszkiewicz, J., & Czerny, B., 2001, *New Astronomy*, in press (astro-ph/0104263)
- Merritt, D. 1997, *AJ*, 114, 228
- Merritt, D., & Ferrarese, L. 2001a, *ApJ*, 547, 140 (MF01a)
- Merritt, D., & Ferrarese, L. 2001b, *MNRAS*, 320, L30
- Milosavljevic, M. & Merritt, D. 2001, *astro-ph/0103350*
- Nelson, C., & Whittle, D.M. 1995, *ApJS*, 99, 67 (NW95)
- Netzer, H., & Peterson, B.M. 1997, in *Astronomical Time Series*, ed. D. Maoz, A. Sternberg, & E.M. Leibowitz, (Dordrecht: Kluwer), p. 85
- Peterson, B.M. 1993, *PASP*, 105, 247
- Peterson, B.M., et al. 2000, *ApJ*, 542, 161
- Peterson, B.M., & Wandel, A. 2000, *ApJ*, 540, L13
- Pogge, R.W. 1992, in *CCD Observing and Reduction Techniques*, ed. S.B. Howell, (San Francisco: Astronomical Society of the Pacific), p. 195
- Richstone, D., et al. 1998, *Nature*, 395, A14
- Silk, J., & Rees, M. 1998, *A&A*, 331, 1
- Smith, E.P., Heckman, T.M., & Illingworth, G.D. 1990, *ApJ*, 356, 399
- Wandel, A., Peterson, B.M., & Malkan, M.A. 1999, *ApJ*, 526, 579
- Wandel, A. 1999, *ApJ*, 519, L39